

CHARACTERIZATION OF IRON OXIDES FROM ABANDONED MINE DRAINAGE DISCHARGES¹

C.A. Neely² and R.W. Nairn

Abstract. This study characterizes mine-drainage derived iron oxides as a precursor for the determination of potential reuses in sustainable water treatment processes. Pure iron oxides have been established as an effective sorptive media or coating for water treatment, yet iron oxides from mine drainages have largely been ignored as a source for this raw material. In addition to passive mine drainage treatment systems, environmental discharges of mine water and associated iron deposits were also examined. In total 13 sources of iron oxides were collected, these sources include 12 coal mining related discharges and one hard rock mining discharge. Water quality and dissolved metals data for the mine water were analyzed to aid in correlating site specific mine water conditions and dominant form of iron oxide present at each location. The iron characterization consisted of X-ray diffraction (XRD) analysis to determine the dominant form of iron, Munsell color classification, particle density, loss on ignition (LOI) to estimate organic matter, scanning electron microscopy (SEM) analysis to determine individual particle size, dry sieve particle size distribution (PSD) to attain ASTM particle size classifications, Brunauer-Emmett-Teller (BET) analysis of surface area, acid oxalate digestions (AOD) to determine the percent of crystalline and non-crystalline material, and inductively coupled plasma-optical emission spectroscopy (ICP-OES) analysis for metal concentrations in each iron oxide sample. Observed ranges of selected parameters are: Munsell color (5YR – 10YR); particle density (1.97 – 3.04 g/cm³); LOI (0.59 – 1.41%); SEM of smallest individual particles (5 – 20 nm); BET surface area (63.75 – 497.02 m²/g); AOD (13.52 – 96.31% non-crystalline material); and the iron content obtained from ICP-OES analysis ranged from (47 to 94% as goethite). The information gained through this detailed characterization of mine-drainage derived iron oxides may eventually aid in the future selection of appropriate iron oxides for sustainable reuse in water treatment processes.

Additional Key Words: Passive Treatment, Environmental Discharge, Goethite

¹ Paper was presented at the 2010 National Meeting of the American Society of Mining and Reclamation, Pittsburgh, PA *Bridging Reclamation, Science and the Community* June 5 - 11, 2010. R.I. Barnhisel (Ed.) Published by ASMR, 3134 Montavesta Rd., Lexington, KY 40502.

² Cody A. Neely, Graduate Research Assistant and Robert W. Nairn, Associate Professor, Center for the Restoration of Ecosystems and Watersheds, School of Civil Engineering & Environmental Science, University of Oklahoma, Norman, OK 73019.

Proceedings American Society of Mining and Reclamation, 2010 pp 691-721

DOI: 10.21000/JASMR10010691

<http://dx.doi.org/10.21000/JASMR10010691>

Introduction

In recent years passive mine drainage treatment systems have served as an effective means of improving water quality for areas that have been negatively impacted by abandoned mining operations (e.g., Nairn et al., 2009). Consequently, these passive treatment systems accumulate metal precipitates throughout their design life. Specific unit processes are designed to maximize metal removal while serving as an impoundment to retain waste material until removal is deemed necessary for the system to function properly. Oxidation ponds are utilized to remove iron in the form of iron oxides, while vertical flow bioreactors are applied to remove trace metals as metal sulfides and to generate alkalinity (Watzlaf et al., 2004). To this point in time, the prominent train of thought with respect to the disposal of these waste by-products is via excavation and consequential landfilling as a controlled or special waste (Wiseman and Edwards, 2004). The disposal of these waste by-products only requires action to be taken once a treatment system reaches its designed carrying capacity of accumulated waste materials (typically 10-30 years). Currently there is a great deal of interest in determining if these passive treatment systems' waste by-products can be recovered and beneficially reused as a raw material in other lines of production (e.g., Hedin, 1999). Additionally, it remains a possibility that the revenue generated from the sale of these by-products could play an important role in supplementing the operation and maintenance costs of passive treatment systems to extend their operational design life.

Interests in the possibility of recovering and reusing iron oxides from acid mine drainage began to emerge in the mid 1990's. One of the pioneers in this advancement was Robert Hedin, who was granted a U.S. Patent in 1999 for the production of "pigment-grade iron oxides" from polluted acid mine drainages (Hedin, 2002). The research that Hedin conducted was centered in western Pennsylvania where the primary source of the acid mine drainage originates from the numerous abandoned coal mining operations that litter the landscape. The site that produced the first acid mine drainage recovered iron oxides is located near the town of Lowber, PA. All that remains of the previous mining operation, coal processing, and coking facility in Lowber is merely an abandoned deep mine and a drainage channel leading to Sewickley Creek that had accumulated nearly 60 years worth of iron rich sludge, which was successfully extracted, dewatered, and sold to a customer in the pigment industry (Hedin, 2002). This project confirmed the feasibility of iron recovery from acid mine drainage; however, advancements to make this process more efficient and therefore more profitable are still in process today.

As global environmental awareness continues to heighten, there is an increase in the implementation of treatment systems to improve the water quality of abandoned mine drainages. This in turn provides three major sources that can be utilized to recover the resulting immense stock of accumulated iron oxides. Passive and conventional active mine drainage treatment systems are continually accumulating large quantities of metals (such as iron oxides) while treating their respective influent mine drainage source waters. In addition to established treatment systems, there are many untreated abandoned mine drainage discharges occurring in the environment that may contain decades of accumulated iron oxides. In fact, it has been estimated that annually over 100,000 tons of iron are discharged from coal mines in the United States alone (Hedin, 1996). The large quantities of iron oxides that are accumulating as waste by-products potentially represent a major sustainable source of raw material that can be reused.

The potential reuses of iron oxides are not solely limited to the production of pigments. Iron oxides are known to be commonly used in cosmetics, pottery glazes, soil remediation technologies, sorptive filtration media and coatings (for removing cations or anions depending upon the pH of solution with respect to point of zero charge), phosphate and metals retention, and animal feed additives (Boujelben et al., 2008; Dzombak and Morel, 1990; Heal et al., 2005; Penn et al., 2007; Kang et al., 2003; Wei et al., 2008; Sibrell et al., 2009). There is a notable distinction that could play a crucial role in limiting the use of recovered iron oxides. This aspect lies in the relative purity of the iron oxide. Iron oxide purity largely depends on the type of mining operation from which the mine drainage originates. Generally hard-rock mining drainages contain higher levels of trace metals (which originally were the focus of the mining) than that which coal-mine drainages possess (Wildeman et al., 1994).

Typical impurities that have been found in recovered iron oxides consist of: sodium (Na), magnesium (Mg), potassium (K), calcium (Ca), aluminum (Al), manganese (Mn), arsenic (As), cobalt (Co), cadmium (Cd), chromium (Cr), nickel (Ni), lead (Pb), and zinc (Zn). In general, concentrations of these impurities can range from tens of mg/kg to thousands of mg/kg depending on site-specific geology and water quality characteristics (Kairies et al., 2005). If the recovered iron oxide product contains elevated levels of toxic metals such as Pb, As, Cd, Cr, Zn or Ni it may not be suitable for use in products consumed by animals, or products in which the toxic heavy metals (even at modest exposure levels) could pose a health risk to humans (Yu, 2005).

This paper describes the detailed characterization of 13 mine-drainage derived iron oxides. This characterization was performed in effort to identify the intrinsic properties that recovered iron oxides exhibit. Examination of such characteristics is an important aspect in determining the potential reuse options available for deposits of mine-drainage derived iron oxides.

Site Locations

Abandoned mine drainage site locations were selected based on available water quality criteria. Mine drainage discharges of varying pH were desired since pH is a critical factor in formation of individual phases of iron oxides. Iron oxide precipitates such as goethite (α -FeOOH), lepidocrocite (γ -FeOOH), schwertmannite ($\text{Fe}_{16}\text{O}_{16}(\text{OH})_y(\text{SO}_4)_z \cdot n\text{H}_2\text{O}$), and ferrihydrite ($\text{Fe}_5\text{HO}_8 \cdot 4\text{H}_2\text{O}$) can typically be found in mine drainage discharges, depending upon the site specific pH conditions (Schwertmann and Cornell, 1991). According to Bigham et al. (1992), schwertmannite is the predominant mineral formed in acidic mine drainages with pH between 3.0 and 4.5, while ferrihydrite and goethite form at pH >5.0 and 6.0, respectively. Bigham et al. (1992) also point out that both schwertmannite and ferrihydrite are meta-stable with respect to goethite and will gradually transform to goethite over time. Generally, significant amounts (2 to 10 percent) of goethite appear in amorphous iron oxide samples after 12 to 15 days of aging (Avotins, 1975; Crosby et al., 1983, Dzombak and Morel, 1990).

Choices for passive treatment system locations are those that the OU Center for Restoration of Ecosystems and Watersheds (CREW) has studied: Mayer Ranch, Hartshorne, Red Oak, and Leboskey. Of these passive treatment systems, only Mayer Ranch receives hard-rock (lead-zinc) mine drainage in northeast Oklahoma, the others all receive coal mine drainage in southeast Oklahoma. The utilization of passive treatment systems serves to provide sampling sites with prior information about the site-specific water quality and aqueous metals composition present at each location. In addition, there are several environmental discharges including the Gowen site (Battles & Burger discharges), Panola Seep #1, Panola Seep #2, Jeffries, Howe, and the Georges Colliers Incorporated (GCI) mining discharge; which are all located in the coal mining region of southeast Oklahoma and were selected as sources of iron oxide recovery for this study. Figure 1 seen below, shows northeast Oklahoma's Mayer Ranch passive treatment system, while Fig. 2 shows southeast Oklahoma's Panola #1 environmental discharge.



Figure 1. Aerial photograph of Mayer Ranch passive treatment system, NE Oklahoma (pH = 6)



Figure 2. Panola Seep #2 environmental discharge, SE Oklahoma (pH = 5)

An additional low pH environmental discharge (Pine Lane, Fig. 3) was collected from a surface mining discharge in the bituminous coal fields located in western Pennsylvania's Clarion County. The historic variability in site-specific water quality parameters from each of these

sampling locations ensures that iron accumulations from circum-neutral, low, and intermediate pH mine water discharges were sampled.



Figure 3. Pine Lane environmental discharge, Western Pennsylvania (pH = 3)

Water Quality

Water quality and aqueous metals data were compiled for each of the sampling locations where the data were available. Some of the environmental discharges were lacking historical water quality data, due to the fact that many of these discharges have gone unmonitored for decades. Table 1 lists the average values of available water quality data from the selected sampling locations (n values range from n=1 for some environmental discharges to n=84 for regularly monitored passive treatment systems).

Table 1. Available water quality data for the chosen sampling locations, expressed in mg/L except where noted

Sample Location	pH su	Alkalinity (mg/L as CaCO ₃)	Temp °C	DO	SO ₄ ²⁻	Al	As	Ca	Cd	Co	Cr	Cu	Fe	Mg	Mn	Na	Ni	Pb	Zn
<i>Passive Treatment Systems</i>																			
Mayer Ranch (n=84)	5.95	400	17.80	1.03	2,160	0.36	0.068	744	0.015	0.058	0.002	0.005	196	201	1.66	97.68	0.957	0.060	10.02
Red Oak (n=13)	6.65	215	17.62	0.67	1,050	0.046	0.040	476	0.011	0.013	0.004	0.003	120	55	5.14	27.26	0.019	0.039	0.016
Hartshorne (n=46)	6.19	469	20.49	1.10	4,920	0.052	0.024	571	0.036	0.049	0.003	0.003	542	230	8.52	1,320	0.042	0.224	0.052
Leboskey (n=5)	6.56	190	20.62	1.80	114	0.048	<0.022	103	0.004	0.004	<0.001	0.002	42.7	9	1.81	6.37	0.057	0.025	0.012
<i>Environmental Discharges</i>																			
Gowen Burgers (n=4)	5.16	33.5	17.51	1.50	920	2.16	<0.022	70	0.017	0.109	0.002	0.002	137	45	6.33	27.88	0.157	0.038	0.234
Gowen Battles (n=6)	3.70	0	17.56	1.51	1,070	53.2	<0.022	87	0.043	0.427	0.020	0.012	303	74	14.22	14.88	0.653	0.083	1.17
Gowen Confluence (n=1)	4.27	0	16.87	8.56	--	12.92	<0.022	52	0.006	0.132	<0.001	<0.001	94.2	34	5.87	22.68	0.214	<0.021	0.359
Howe (n=3)	4.31	0	16.79	2.62	156	2.12	--	--	--	--	--	--	25.5	--	2.34	--	0.09	0.027	0.17
Jeffries (n=3)	~ 2-3	85	19.45	0.40	5,520	0.622	--	261	<0.01	--	<0.005	--	595	250	24.20	--	0.050	<0.1	<0.01
Panola Seep #1 (n=2)	5.03	42.5	22.10	1.09	--	0.250	<0.022	53	0.002	0.037	<0.001	0.001	65.5	51	2.77	12.77	0.043	0.032	0.021
Panola Seep #2 (n=1)	3.08	0	24.63	4.02	--	1.43	<0.022	56	<0.001	0.103	<0.001	<0.001	6.32	52	10.92	13.32	0.056	<0.021	0.052
GCI (n=6)	3.50	0	16.70	0.59	--	35.88	--	136.56	<0.01	--	0.045	<0.04	94.17	--	5.44	--	0.293	<0.1	0.748
Pine Lane (n=1)	3.00	--	--	--	--	--	--	--	--	--	--	--	--	--	--	--	--	--	--

-- no data available

Methods

Sampling & Sample Preparation

For sites where water sampling occurred, water samples were collected in 250-mL HDPE bottles for anions and metals analysis. Anion samples were filtered with 0.20 μ m Millipore nylon filters and passed through Dionex OnGaurd II H cartridges to remove any multivalent cations such as alkaline earth or transition metals that could pass through the 0.20 μ m filters. The Dionex cartridges are utilized to remove matrix interferences caused by dissolved metals in the samples, while consequently extending the column life of the ion chromatograph. The metals samples were field acidified to a pH < 2 with trace metal grade HNO₃ to ensure that the dissolved metals will not precipitate from solution. Water quality parameters (pH, temperature, DO, etc.) were recorded in the field using a YSI 600QS multiparameter datasonde with YSI 650 display. Field alkalinity measurements were determined using the Hach digital titration method 8203 (APHA, 2005).

Samples of iron oxide precipitates were taken as grab samples from each location. A shovel was used to aid in the collection of the iron oxide samples. As the samples were collected they were stored in 1-L sealable plastic bags to be taken back to the laboratory. The shovel was thoroughly washed with deionized water between each sampling location. Upon arrival in the laboratory the samples were frozen to later be freeze dried at a vacuum of 10 microns of mercury and a vessel temperature of -40°C with a Labconco, model 77500 FreeZone 4.5L benchtop freeze dry system. Freeze drying was utilized in order to avoid any phase transformations that could occur (especially with ferrihydrite) during a conventional air or oven drying process (Schwertmann and Cornell, 1991). Once dry, any aggregates in the samples were manually broken apart before being passed through sieves of appropriate sizes to remove any visible organic debris.

Physical & Chemical Analysis

Anion analyses of the water samples were performed at the University of Oklahoma's CREW laboratory using a Metrohm 761 Ion Chromatograph and following the procedures of EPA method 300; whereas the aqueous metal samples were microwave digested according to EPA method 3015 and analyzed on a Varian Vista-Pro Inductively-Coupled Plasma-Optical Emission Spectrometer (ICP-OES) according to the EPA method 6010 in the same laboratory

(US EPA, 2009). Metals analysis of the iron oxide solids were also performed in the CREW laboratory where the solid samples were subjected to microwave digestion according to EPA method 3051a and analyzed on the ICP-OES via EPA method 6010 (US EPA, 2009).

X-ray diffraction (XRD) and specific surface area determinations were performed at the OU Physical and Environmental Geochemistry Laboratory. The XRD analyses were performed as smear mounts on a Rigaku D-Max powder X-ray diffractometer with a Cu X-ray source and a post-sample curved graphite monochromator. Resulting XRD peaks and patterns were matched to an existing database using the JADE software package. Specific surface area analyses of two distinct particle size fractions ($< 75 \mu\text{m}$ and $75\text{-}106 \mu\text{m}$) were performed by nitrogen gas adsorption using a Beckman-Coulter SA3100 Surface Area and Pore Size Analyzer. Iron oxide powders were carefully weighed in their specimen holders and outgassed at 25°C for 24 hours under vacuum. After outgassing was complete, the samples were quickly capped with rubber stoppers, weighed, and subjected to analysis. Specific surface area was determined by the 5-point B.E.T. method (Brunauer et al., 1938) over the pressure range P/P_0 0.05-0.2. Freespace determinations were performed using ultrapure helium (He). Measured pressures were constantly referenced against a separate cell.

Particle size and surface morphology were analyzed at the OU Samuel Roberts Noble Electron Microscopy Laboratory where a JEOL JSM-880 scanning electron microscope (SEM) with an accelerating voltage of 15 kV was used to generate micrographs of the iron oxide samples. The samples were prepped by sputter coating them with approximately 5nm of a 60-40 gold palladium (AgPd) alloy using an Anatech Ltd. Hummer VI sputter coater. Micrographs of several magnifications were taken for each sample in order to capture the array of particle sizes that were present, while still allowing for the inspection of individual crystalline structures. Additionally, a particle size distribution (PSD) was performed on each sample to provide traditional American Society for Testing Materials (ASTM) classification criteria. The following sieve sizes (#60, #100, #140, #200, #270, #325, and collection pan) were utilized in the size separation of 25.0000 g of sample by manual shaking for 3 minutes. A sieve duration of 3 minutes was strictly upheld due to the friable nature of the iron oxide powders, which Klute (1986) identify as an adequate amount of time to size separate friable substances. After 3 minutes of shaking, the friable particles were allowed to settle for 1 minute and the mass of sample caught on each screen was carefully weighed on an analytical balance to 4 decimal

places. Once the sieve analyses were completed, MATLAB software version 7.4.0.287 (R2007a) was used to run the SieveAnalysis5 program to generate traditional PSD graphical data and classifications.

Particle density, color classification, organic matter content, water content, and percent crystallinity account for the rest of the characterization parameters that were analyzed. These analyses were conducted in the OU CREW laboratory. Density was determined according to the 1958 manual pycnometer method described by the American Society for Testing and Materials. Iron oxide color classifications were performed with dry powders passing mesh sieve screens (#60 and #200) and classified according to the Munsell Soil Color (2000) procedure. Two differently sized sieves were used to show any color variations that occur when passed through smaller restrictive openings. Organic matter and water content analyses were performed according to the loss on ignition (LOI) and gravimetric water content methods described in Ben-Dor and Banin (1989). This method involves first oven drying 1.0000 g of sample at 105°C for 24 hours followed by cooling in a desiccator, which yields the water content of the sample. Next, the LOI is determined by igniting the samples in a muffle furnace at 400°C for 16 hours. The observed reductions in weight represent the LOI, and are assumed to equal the organic matter content of each sample. Minimal error is incorporated into this assumption due to the presence of structural water and other components that may be volatilized during analysis. Lastly, percent crystallinity was determined through acid oxalate extractions performed in the dark (AOD) according to the method described in Schwertmann and Cornell (1991). The AOD analysis was performed using 250-mL amber HDPE bottles to exclude any light from influencing the reactions. The AOD method consisted of taking 0.250 g of sample, adding 50 mL of 0.2M ammonium oxalate to the reaction vessel capping it and placing it on a reciprocating shaker for two hours. After shaking, the samples were centrifuged and the supernatant was decanted, and the sample was then washed three times with 0.5M ammonium carbonate. Next the sample was washed with a volume of water that was equal to volume of ammonium carbonate. The sample was then dried overnight at 110 °C; allowed to cool to room temperature and then the final weight was recorded. From the difference in initial and final weights it can be determined what percent of the sample is crystalline in nature, due to the fact that the amorphous iron is dissolved during this procedure while crystalline goethite and hematite are essentially left un-dissolved (Schwertmann and Cornell, 1991).

Results

Color, Moisture, & Organic Matter

The unique ochre colored tones that iron oxides possess are one of the first characteristics observed when dealing with the collection of mine drainage precipitates. Table 2 displays the comparison of Munsell Color classifications for each iron oxide sample at particle sizes passing both #60 and #200 sieves, exemplifying any variations in color that occur when passing different screen sizes. Figure 4 shows the range of colors exhibited by the iron oxides after being passed through the #200 sieve. The range of water content (after freeze drying) in the collected iron oxide samples varied from 2 to 9 percent. Percent organic matter content for iron oxides passing a #200 sieve also displayed a narrow range of values spanning from 0.59% (± 0.03 standard deviation) for Leboskey to 1.41% (± 0.04) in the Pine Lane sample.

Table 2. Munsell Color classification of iron oxide samples

Sample Name	Munsell Color Classification (Passing #60 Sieve)				Munsell Color Classification (Passing #200 Sieve)			
	Hue	Value	Chroma	Munsell Color Name	Hue	Value	Chroma	Munsell Color Name
<i>Passive Treatment Systems</i>								
Mayer Ranch	5 YR	4	6	Yellowish Red	5 YR	5	8	Yellowish Red
Red Oak	5 YR	4	6	Yellowish Red	5 YR	5	8	Yellowish Red
Hartshorne	5 YR	5	8	Yellowish Red	5 YR	5	6	Yellowish Red
Leboskey	7.5 YR	5	8	Strong Brown	7.5 YR	5	6	Strong Brown
<i>Environmental Discharges</i>								
Gowen Burgers Seep	10 YR	5	8	Yellowish Brown	10 YR	5	8	Yellowish Brown
Gowen Battles Seep	10 YR	4	6	Dark Yellowish Brown	7.5 YR	4	6	Strong Brown
Gowen Confluence	10 YR	5	6	Yellowish Brown	10 YR	5	8	Yellowish Brown
Howe	5 YR	4	6	Yellowish Red	7.5 YR	5	8	Strong Brown
Jeffries	10 YR	6	8	Brownish Yellow	10 YR	6	8	Brownish Yellow
Panola Seep #1	5 YR	5	8	Yellowish Red	7.5 YR	5	8	Strong Brown
Panola Seep #2	10 YR	4	6	Dark Yellowish Brown	10 YR	5	8	Yellowish Brown
GCI	10 YR	5	8	Yellowish Brown	10 YR	5	8	Yellowish Brown
Pine Lane	7.5 YR	4	6	Strong Brown	7.5 YR	4	6	Strong Brown



Figure 4. Color variations of mine-drainage derived iron oxides after passing a #200 sieve. Numbers correspond to the following samples: (1) Mayer Ranch (2) Gowen Burgers Seep (3) GCI (4) Hartshorne (5) Howe (6) Red Oak (7) Panola Seep #1 (8) Panola Seep #2 (9) Jeffries (10) Leboskey (11) Gowen Battles Seep (12) Gowen Confluence (13) Pine Lane

Particle Density, Crystallinity, & Surface Area.

Particle density values of the dried iron oxides range from $1.97 (\pm 0.03) \text{ g/cm}^3$ at the Hartshorne passive treatment system to $3.04 (\pm 0.02) \text{ g/cm}^3$ at the Jeffries environmental discharge. Altogether the iron oxide samples possessed an average density of $2.51 (\pm 0.31) \text{ g/cm}^3$, which is comparable to particle density values of other naturally occurring iron oxides. Fenton et al. (2009) is one of the few authors that have published data on the particle density of iron oxides from an abandoned mining operation. The particle density that they report ($2.30 \pm 0.53 \text{ g/cm}^3$) is representative of an abandoned Cu-S mine in the Avoca-Avonmore catchment, Ireland. Table 3 shows the respective particle density and standard deviation ($n=3$) of each iron oxide sample collected for the current study. The percent crystallinity of each iron oxide sample is shown in Fig. 5. Crystallinity values ranged from 3 to 86% for Howe and Pine Lane, respectively. Specific surface area results for the particles $< 75 \mu\text{m}$ showed a wide range of values spanning from $63 \text{ m}^2\text{g}^{-1}$ at Gowen Battles Seep to

497 m²g⁻¹ at Panola Seep #2. When considering all samples, the average BET specific surface area was 175 m²g⁻¹. The 75 to 106 µm particle sizes possessed a BET specific surface areas ranging from 58 m²g⁻¹ at Gowen Battles Seep to 267 m²g⁻¹ at Mayer Ranch passive treatment system. The average BET specific surface area for all samples at this larger size fraction was calculated to be 142 m²g⁻¹. The relationship between each iron oxide sample and its respective surface area for each size fraction is displayed in Fig. 6.

Table 3. Mean particle density and standard deviation of mine drainage derived iron oxides (n=3)

Sample Name	Mean Particle Density (g/cm ³)	Standard Deviation
<i>Passive Treatment Systems</i>		
Mayer Ranch	2.39	± 0.0014
Red Oak	2.31	± 0.0087
Hartshorne	1.97	± 0.0279
Leboskey	2.55	± 0.0489
<i>Environmental Discharges</i>		
Gowen Burgers Seep	2.12	± 0.0029
Gowen Confluence	2.59	± 0.0137
Gowen Battles Seep	2.43	± 0.0114
Howe	2.60	± 0.0032
Jeffries	3.04	± 0.0158
Panola Seep #1	2.59	± 0.0620
Panola Seep #2	2.82	± 0.0441
GCI	2.26	± 0.0045
Pine Lane	2.91	± 0.0077

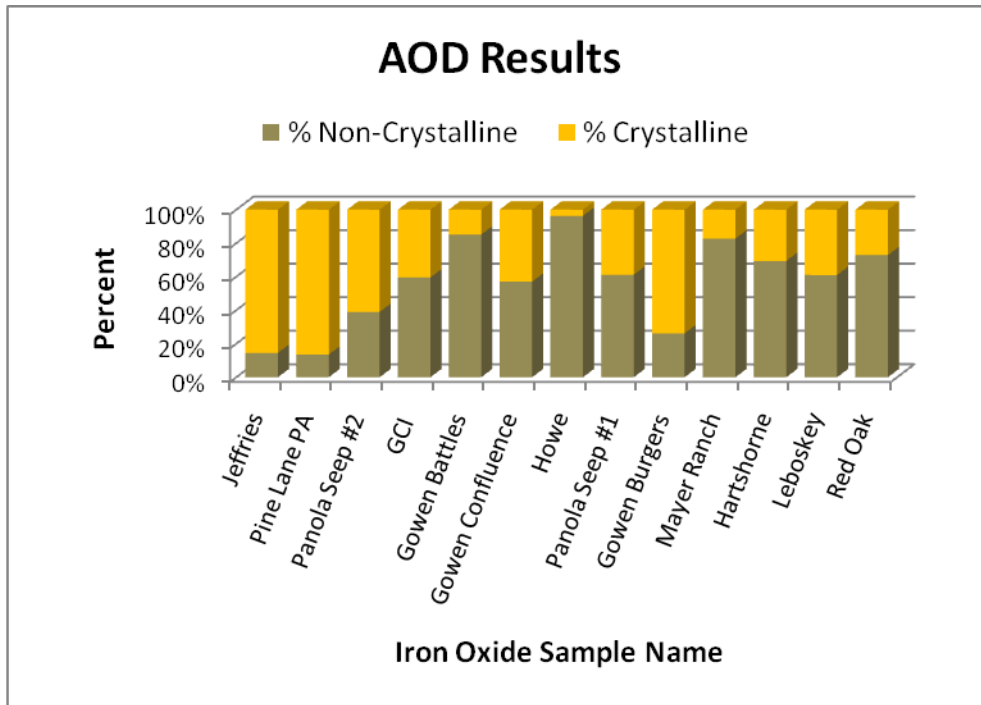


Figure 5. Crystallinity of mine drainage derived iron oxides

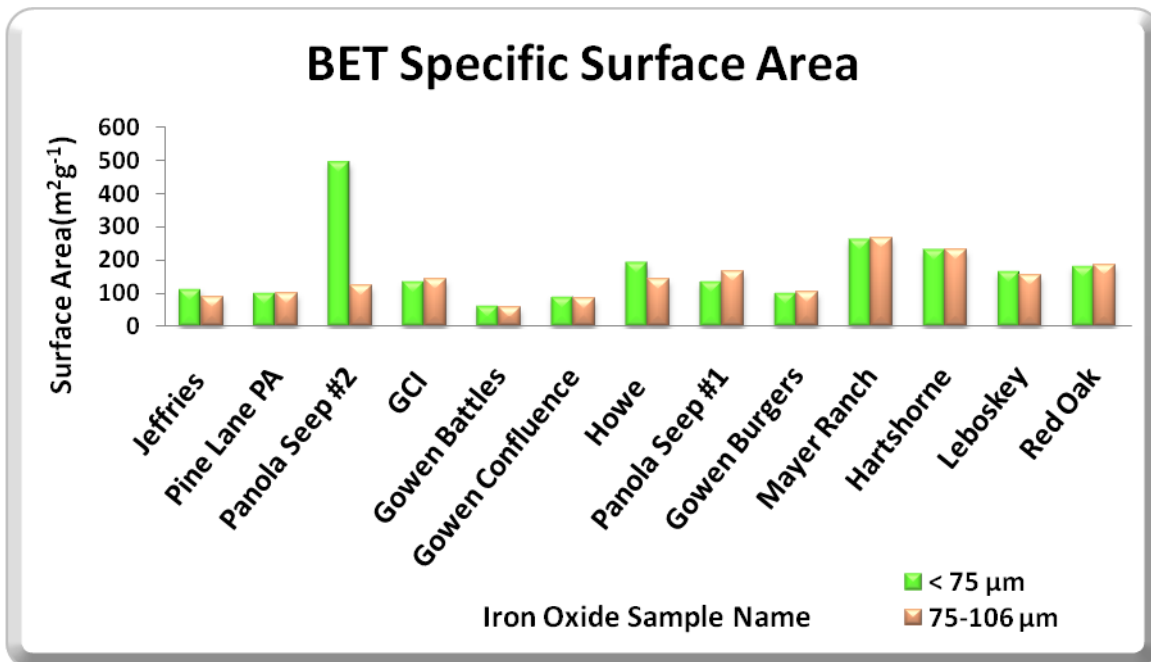


Figure 6. Specific surface area of mine drainage derived iron oxides

Particle Size, Morphology, & Mineralogy

Particle size distribution and identification of surface morphology characteristics of the iron oxide precipitates were determined through a combination of SEM observation and PSD sieve analyses. The PSD analyses proved that all samples contained the same ASTM particle size classification ‘fine sand’. Table 4 includes a more specific dissection of the data indicating the parameters of interest, such as D_{10} , D_{50} , and mean grain size. The smallest individual particles making up each sample were observed by SEM to range between 5 and 20 nm in diameter. From the PSD results semi-log cumulative probability curves were plotted for each sample. Due to the fact that the cumulative probability curves appear to be similar, the curve for Mayer Ranch passive treatment system was selected to be representative of the group and is displayed in Fig. 7. The surface morphology of these iron oxides were observed to be primarily globular with some instances of acicular, platy, and spiky (or ‘hedge-hog’) shaped structures of iron oxide. Figure 9 illustrates the surface morphology types observed from these mine drainage derived iron oxides. XRD analyses performed on the samples showed the predominant phase of iron in all samples was goethite. Results from the XRD analyses, including the identification of possible minor iron oxide phases are shown in Table 5, and example XRD diffractograms from select mine drainage derived iron oxides are displayed in Fig. 8 (A, B, C, D).

Table 4. Particle size distribution findings including D_{10} , D_{50} , mean grain size, and ASTM classification.

Sample Name	ASTM Classification	D_{50} μm	D_{10} μm	Mean Grain Size μm
<i>Treatment Systems</i>				
Mayer Ranch	Fine Sand	85.8	52.0	94.0
Red Oak	Fine Sand	77.6	51.4	87.7
Hartshorne	Fine Sand	92.4	60.7	101.6
Leboskey	Fine Sand	108.3	74.8	117.9
<i>Environmental Discharges</i>				
Gowen Burgers Seep	Fine Sand	92.4	58.1	100.2
Gowen Confluence	Fine Sand	77.3	52.9	86.4
Gowen Battles Seep	Fine Sand	103.9	49.3	100.7
Howe	Fine Sand	84.7	50.3	92.8
Jeffries Field	Fine Sand	126.6	89.2	129.4
Panola Seep #1	Fine Sand	71.0	54.5	81.0
Panola Seep #2	Fine Sand	98.8	48.8	102.1
GCI	Fine Sand	97.7	53.0	102.9
Pine Lane	Fine Sand	95.8	49.4	97.7

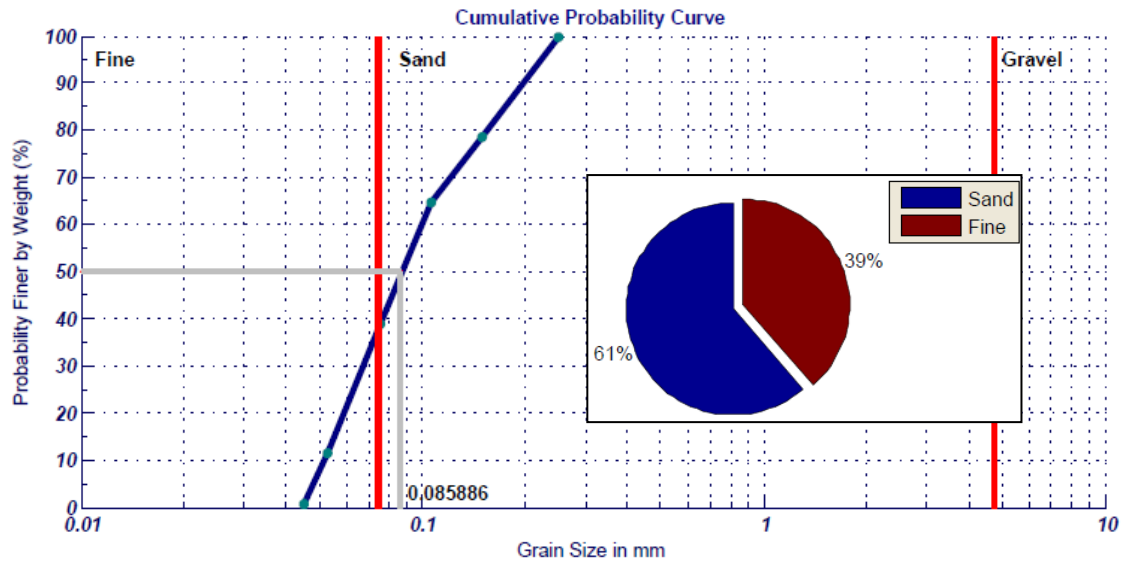


Figure 7. Mayer Ranch passive treatment system PSD cumulative probability curve with D_{50} , ASTM classifications, and percent sand/fines denoted.

Table 5. Mineralogy of mine drainage derived iron oxides

Sample Name	Dominant Phase	Possible Minor Phases
<i>Treatment Systems</i>		
Mayer Ranch	Goethite	Akaganeite, Magnetite
Red Oak	Goethite	Hematite
Hartshorne	Goethite	Hematite
Leboskey	Goethite	
<i>Environmental Discharges</i>		
Gowen Burgers	Goethite	
Gowen Battles Seep	Goethite	
Gowen Confluence	Goethite	Ferrihydrite (6-line)
Howe	Goethite	Magnetite, Jarosite, Maghemite
Jeffries	Goethite	Jarosite, Ferrihydrite (6-line)
Panola Seep #1	Goethite	Ferrihydrite (6-line), Maghemite
Panola Seep #2	Goethite	Magnetite
GCI	Goethite	Akaganeite, Lepidocrocite
Pine Lane	Goethite	Hematite, Akaganeite

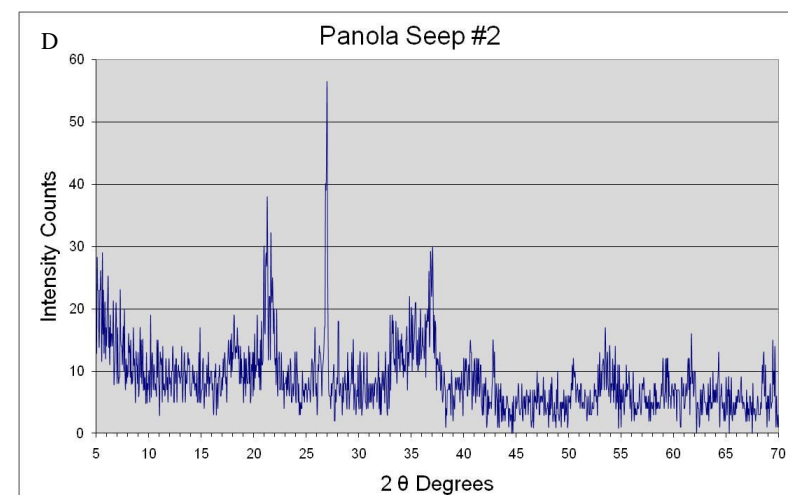
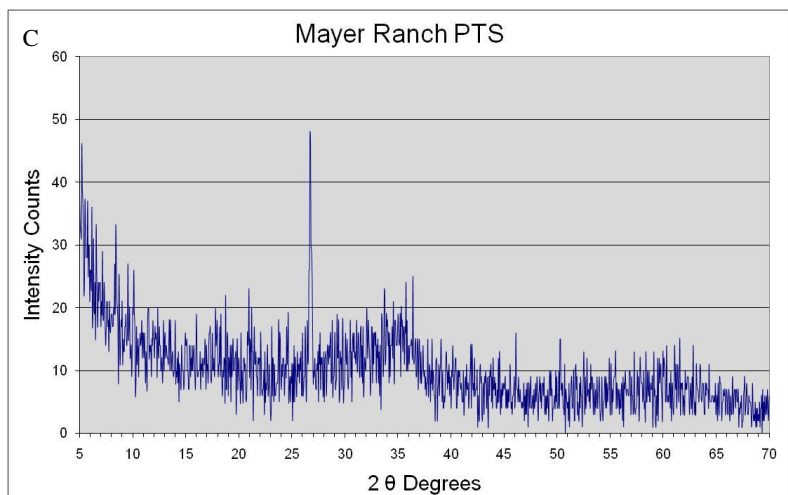
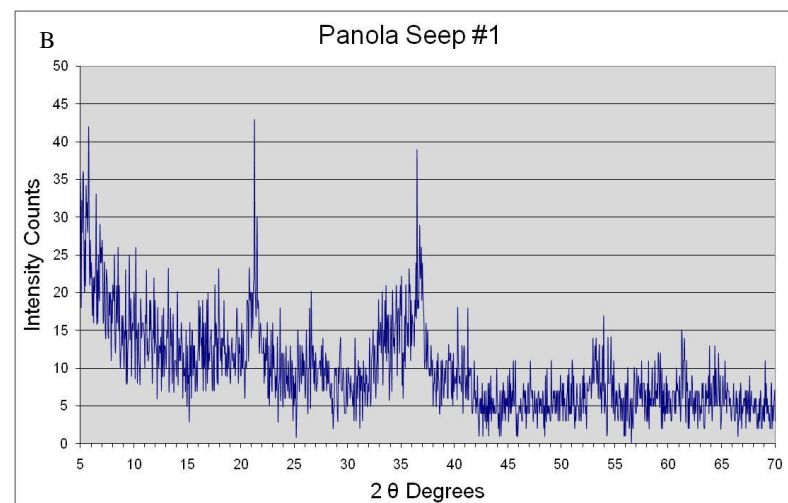
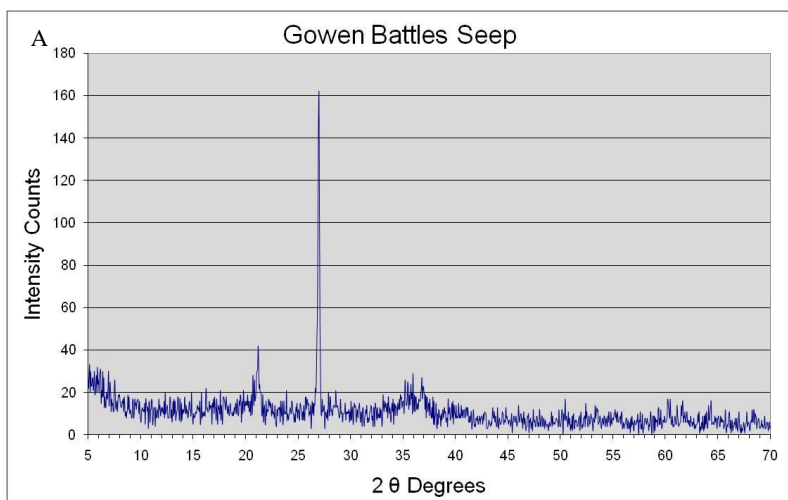


Figure 8. XRD diffractograms from select mine drainage derived iron oxides (A) Gowen Battles Seep (B) Panola Seep #1 (C) Mayer Ranch Passive Treatment System (D) Panola Seep #2

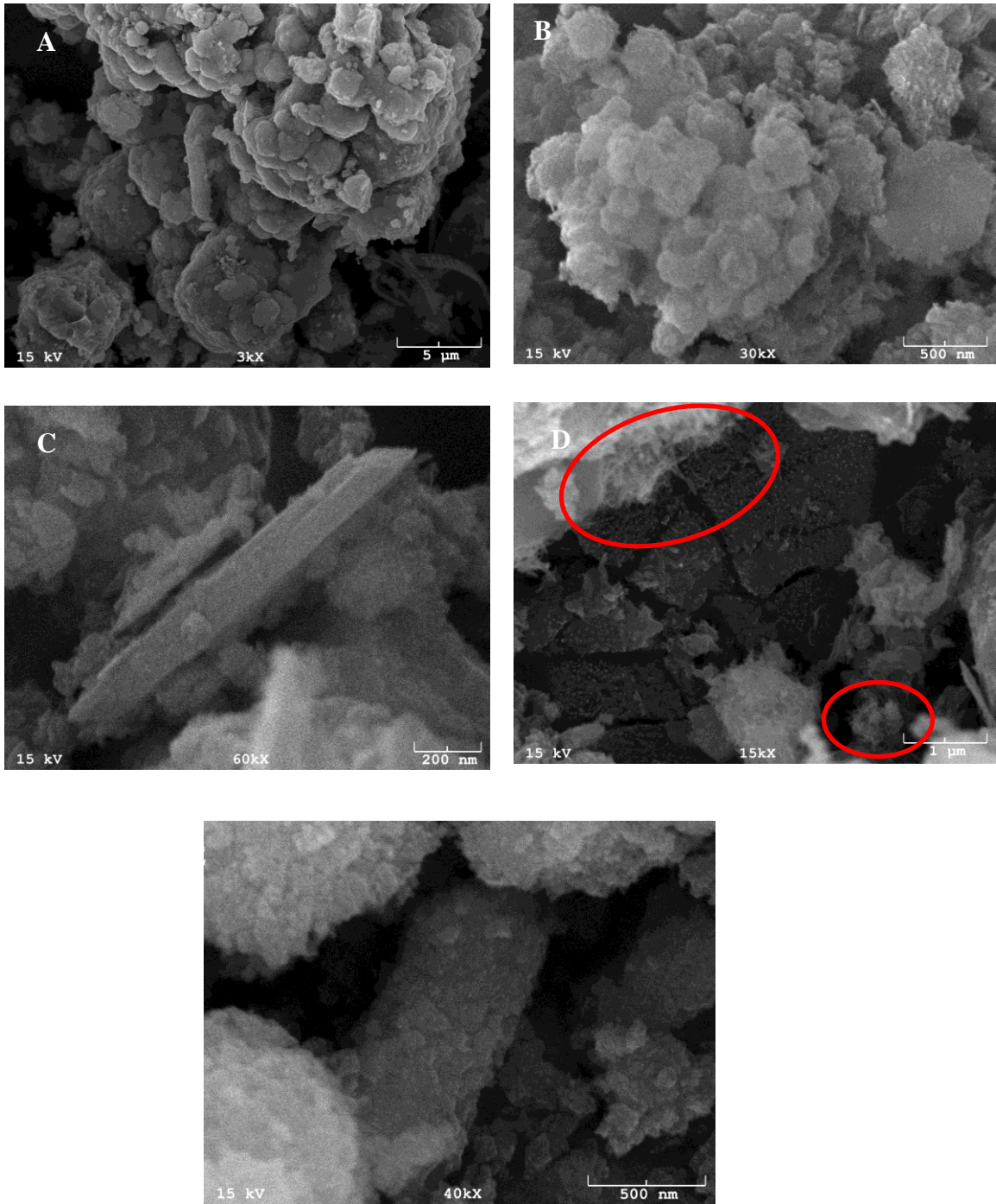


Figure 9. Types of iron oxide morphology observed in SEM micrographs: (A & B) Globular, (C) Acicular, (D) Spiky, (E) Platy. Spiky morphology is typical of schwertmannite, and can be seen as the circled structures in (D).

Precipitate Chemistry

Metal concentrations (in mg/kg) were determined for all iron oxide samples via ICP-OES analysis. This analysis aids in the identification of impurities that are incorporated into the structure of each mine drainage derived iron oxide sample. Since goethite was the predominant form of iron oxide identified in all samples, the iron content has been represented as percent α -FeOOH for display in Table 6. A comprehensive evaluation of existing impurities found in each of the 13 iron oxide samples is provided in Table 7.

Table 6. Percent iron oxide as α -FeOOH

Sample Location	Iron (mg/kg)	% (α -FeOOH)
Mayer Ranch	469,650	74.72
Red Oak	592,150	94.20
Hartshorne	572,070	91.01
Leboskey	303,340	48.26
Gowen Burgers	428,060	68.10
Gowen Battles	391,130	62.22
Gowen Confluence	333,750	53.10
Howe	531,480	84.55
Jeffries	451,450	71.82
Panola Seep 1	572,550	91.09
Panola Seep 2	447,760	71.23
GCI	300,880	47.87
Pine Lane	540,750	86.03

Table 7. Metal constituents of iron oxide precipitates in mg/kg

Sample Location	Al	As	Ca	Cd	Co	Cr	Cu	Fe	K	Mg	Mn	Na	Ni	Pb	Zn
Mayer Ranch	1,610	459	24,940	45.4	26.7	2.79	10.4	469,650	502	1,010	267	352	217	188	6,360
Red Oak	88.3	359	2,930	53.4	22.7	1.73	5.78	592,150	334	143	853	< DL	105	216	46.2
Hartshorne	269	37.2	13,730	47.7	19.6	1.83	9.50	572,070	575	1,010	366	3,050	91.0	206	44.1
Leboskey	4,160	52.6	5,730	26.7	89.6	6.35	16.3	303,340	886	412	6,046	< DL	103	122	60.6
Gowen Burgers	4,210	37.9	654	38.6	21.7	32.6	16.3	428,060	694	404	292	385	81.0	164	100
Gowen Battles	6,290	22.7	184	32.8	18.5	55.5	22.5	391,130	630	169	180	< DL	69.8	140	63.5
Gowen Confluence	6,340	19.4	220	30.4	18.4	31.7	12.2	333,750	727	343	184	< DL	62.6	135	64.5
Howe	1,240	11.7	324	46.0	18.5	2.35	8.01	531,480	485	214	237	< DL	89.1	195	70.0
Jeffries	1,500	10.2	705	38.3	16.4	5.19	24.8	451,450	9,390	427	218	1,960	73.0	171	39.4
Panola Seep 1	1,410	107	199	51.5	18.4	2.11	3.00	572,550	334	152	254	< DL	93.8	206	53.1
Panola Seep 2	2,370	71.6	171	40.7	17.1	5.92	13.5	447,760	685	286	210	< DL	79.3	172	63.7
GCI	18,380	27.4	1,050	26.1	19.5	74.3	33.7	300,880	676	438	171	< DL	58.6	119	115
Pine Lane	368	6.9	186	45.8	17.7	4.70	44.1	540,750	1,710	116	292	< DL	88.1	191	103

< DL stands for below detection limit: Na (0.129 mg/kg)

Discussion

Color & Organic Matter

The color of iron oxides has made them a prominent pigment used to produce colors such as Venetian red, yellow ochre, and burnt Siena among others. In terms of Munsell color classifications, iron oxides can vary greatly in color. Hematite is characteristically bright red in color varying from 5R – 2.5 YR, while goethite is yellowish brown in color ranging from 7.5YR – 10YR. Other forms of iron oxide such as ferrihydrite and lepidocrocite are a mixture of orange, red, yellow and brown that has been noted to have Munsell color classifications from 5YR – 7.5YR (Schwertmann and Cornell, 1991). The colors described in Table 2 and pictured in Figure 4 are within the ranges of these previously described iron oxides. A slight change in color was observed when passing the samples through different mesh sizes. This change in color was noted to undergo a gradual lightening when passed through the #200 mesh. This change is most likely associated with the removal of fine organic debris that was removed by the smaller mesh size, thus removing their associated color contribution from the samples. Particle size, morphology, level of chemical impurities, and the nature of precipitate formation have been suggested by Schwertmann and Cornell (1991) and Cornell and Schwertmann (2003) to influence color. Notably it is mentioned that naturally occurring iron oxides are often cemented into dense masses which appear darker than when they are viewed as dry powders. This specific scenario was observed upon collection of these iron oxides. All samples (even the ones collected from passive treatment systems) exhibited a lightening in color from collection to when they were viewed as dried powders.

Organic matter content determination showed that the samples collected from passive treatment systems contained a slightly lower level of organic matter averaging 0.6% as compared to the environmental discharges which averaged an organic matter content of 1.0%. This result is not surprising due to the fact that the environmental discharges were occurring in areas with significant leaf/pine needle litter that was iron-coated and incorporated into the samples. Even after sieving to remove organic debris, these samples proved to contain a higher level of organic matter due to where they were formed and collected. The samples collected from passive treatment system were typically removed from water submerged areas where little vegetation and organic litter were present. The only noticeable vegetation present at these locations were the *Typha* spp. stands growing along the edges of the treatment systems' ponds, accounting for one

of the few sources of organic matter. Additionally, it remains a possibility that iron oxidizing bacteria such as *Acidothiobacillus ferrooxidans* (Miot et al., 2009) may have been incorporated with the iron oxide samples. The organic cellular components of such microorganisms (although they are likely minor constituents) present a potential source of weight loss during the LOI test.

pH, Density, Surface Area & Crystallinity

Weak associations between pH, particle density, specific surface area, and crystallinity proved to exist when results were plotted against each other and evaluated. These specific parameters are recognized to have important contributions to the chemical and physical makeup of various iron oxide phases. With the exception of Panola Seep #2 (particle size fraction < 75 μm), all specific surface area results were found to increase with increasing mine water pH conditions. Large differences in BET specific surface area, such as that observed between the different size fractions for Panola Seep #2 (497 to 124 m^2g^{-1}) can be explained by the presence of much smaller particles in the < 75 μm sample that likely acted to increase the surface area of that sample. Interestingly, Panola Seep #2 was the only sample that showed a dramatic change in surface area between the different size fractions; suggesting the presence of a greater fraction of fine particles in the <75 μm sample that was analyzed, thus increasing the surface area.

Examples of the weak associations ($r^2 = 0.42$ to 0.56 ; p-values = 0.01 to 0.11) between pH, particle density, surface area, and crystallinity are shown in Fig. 10 (A, B, C, and D). pH vs. particle density (Fig. 10A) shows a linear relationship where the pH of the mine water during formation increases, the density of the iron oxide gradually decreases (Pearson statistical correlation, p-value = 0.02). This suggests that in circum-neutral pH discharges lower density iron oxides such as ferrihydrite may form first then over time transform into the more stable goethite. Such an idea is in accordance with the views that Dzombak and Morel (1990), Avotins (1975), and Crosby et al. (1983) express dealing with the relatively short times (15 days to a month) needed for synthetic amorphous iron oxides such as ferrihydrite to at least partially transition into the more stable goethite. pH vs. surface area (Figure 10D) shows a linear relationship where the surface area increases with increasing pH (p-value= 0.01). This indicates that at higher pH values the formation of amorphous iron oxides are promoted, thus contributing to a higher surface area. The relationship of pH vs. crystallinity (Fig. 10B) is best fit by a second order polynomial line of regression, which describes a higher level of crystallinity in samples that formed in mine water discharges with low pH conditions. Statistically there was not a

correlation since the p-value of 0.09 was above the traditional threshold p-value of 0.05. Particle density vs. crystallinity (Fig. 10C) also is best fit by a second order polynomial line of regression that indicates crystallinity tends to increase as particle density increases. Similarly, the p-value (0.11) of this relationship was slightly above the traditional p-value threshold implying that no statistical correlation exists.

It should be noted that a reason for such weak associations could reside in the fact that many of the samples (especially the environmental discharges) had precipitates that are likely representative of several years. The fact that aging precipitates gradually change into more stable forms is an inherent complication of collecting iron oxides from naturally occurring accumulations (as opposed to synthetic iron oxides). This complication may well factor into poor relationships between these typically important physical parameters.

Particle Size, Morphology, & Mineralogy

Particle size determinations using SEM revealed that the smallest particles present in each of the iron oxide samples were consistently sized at 10-20 nm in diameter, even most globular aggregates were typically less than 5 μm in size. The observed sizes are consistent with those found by Cornell and Schwertmann (2003) where it is stated that iron oxide crystals are usually on the order of 'several nm to a few μm ' in size. Additionally, Avotins (1975) and Crosby et al. (1983) confirm that initially spherical iron oxide particles form with sizes ranging from 1 to 10 nm depending upon pH; however, as they age they coagulate to form aggregates that are typically micrometer sized. The use of SEM was valuable in identifying the smallest fraction of particles that passed through the sieves and were deposited in the sieve pan. The mass of this fraction was deemed insufficient to classify via the traditional hydrometer method, leaving SEM observation as the best option to identify particle sizes in this fraction. PSD results showed that the mean grain size for all samples averaged 99.6 μm in diameter. The ASTM particle size classification for every sample was determined to fit into the 'fine sand' classification. It is interesting to note that only the Panola Seep #1 and Gowen Confluence exhibited D_{50} values that were within the 'fines' ASTM classification, the rest of the samples fit into the 'sand' category.

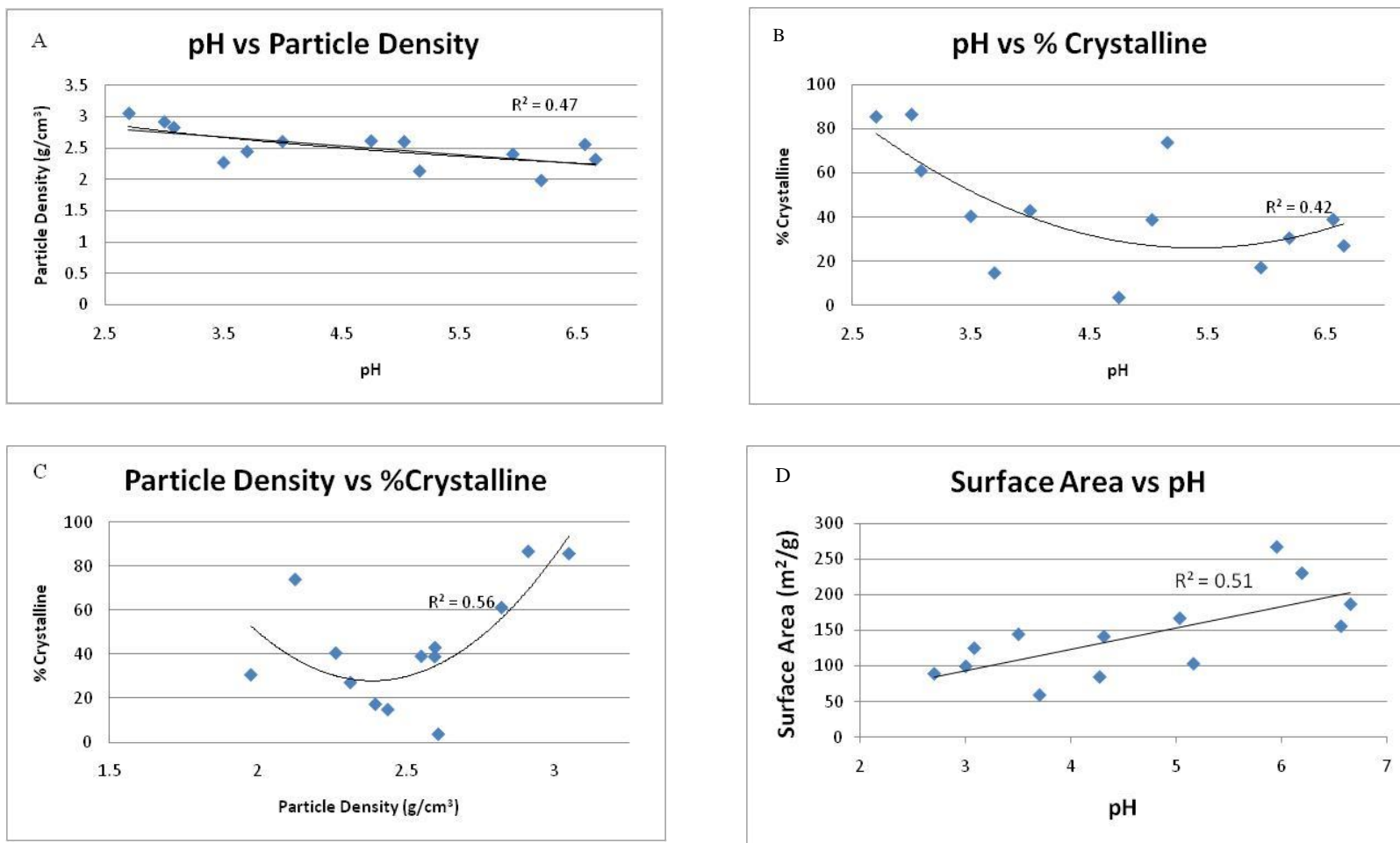


Figure 10. Associations between (A) pH and particle density; (B) pH and crystallinity; (C) crystallinity and particle density and (D) surface area and pH

The SEM analysis also provided micrographs that aided in identifying the morphology and mineralogy of iron oxide samples. The crystal morphologies that were observed throughout these samples are globular, acicular, spiky, and platy. Globular morphologies exist as aggregated iron oxide particles which were observed to range from ~0.5 μm to 5 μm in size. Acicular crystalline structures are characteristic of goethite (Domingo et al., 1994; Schwertmann and Cornell, 1991; Cornell and Schwertmann, 2003, Kairies et al., 2005). Spiky morphology is typical of schwertmannite, and can be seen as the circled structures in Fig. 9D. The identification of schwertmannite through the use of SEM proved to be invaluable since schwertmannite characteristic peaks were not cataloged in the JADE XRD software mineral library. Visual identification confirms the existence of schwertmannite in samples from Panola Seep #2 and Gowen Battles Seep. Platy morphologies are difficult to use for identifying specific types of iron oxide because platy crystals can be characteristic of several different types of iron oxides. Also, impurities in solution can lead to the formation of deformed platy crystals. With these points considered it is also important to denote that hematite and lepidocrocite are traditionally observed as having platy morphologies (Domingo et al., 1994; Cornell and Schwertmann, 2003; Kairies et al., 2005).

Mineralogy was primarily identified through the use of XRD analysis. All samples identified a poorly ordered goethite to be the predominant form of iron oxide present. This is explained by the extended aging period that the precipitates experienced before collection. This aging period would promote the transformation of meta-stable forms of iron oxide to more stable crystalline structures (Cornell and Schwertmann, 2003). Other iron oxides such as ferrihydrite, lepidocrocite, and schwertmannite are capable of being found in the environment because albeit they are thermodynamically less stable, their formation is kinetically favored. Often the complete transformations of meta-stable forms of iron oxides to goethite (with the exception of ferrihydrite) are extremely slow transitioning on a geologic time scale of nearly a thousand years, which helps to explain their presence in the environment (Schwertmann and Cornell, 1991). For this study, the identification of possible minor phases of iron oxides from pre-existing JADE XRD peak patterns proved only to supply possible identifications. Due to the heterogeneous nature of the iron oxide samples, partial matches to several peak configurations were observed. These partial matches are listed as possible minor phases, yet it is important to note that the presence of these iron oxides was not confirmed; but listed as possible constituents. It should

also be noted that other minerals such as various clays, quartz, and pyrite were detected in many of the iron oxide samples, which contributed to the noise and congestion present in the peak configurations obtained from the XRD diffraction patterns.

Precipitate Chemistry

Iron concentrations (mg/kg) for the iron oxides involved in this study suggest that mine drainage derived iron oxides can approach an iron content of 94% (as goethite) with an average iron content of over 72% (as goethite). The samples with lower iron content (47 to 53% as goethite) collected at Leboskey, GCI, and Gowen Confluence were collected at locations where sample contamination from underlying clays was likely due to the relative thickness of accumulated iron. The possibility of these samples containing clay would decrease the iron content of the sample and consequently increase the Al concentration. This idea is supported by the elevated Al content in these samples, suggesting that sample contamination from clay may have occurred. Metal concentrations (mg/kg) observed in the various solid iron oxide samples were noted to at times act unpredictably with respect to the aqueous metal concentrations of the mine water in which they were formed. In many cases when comparing the aqueous metal concentrations of the mining discharge to the metal concentrations in the solid phase, iron oxides showed predictable increases and decreases relative to the level of dissolved metals present in its respective formation environment. Yet at the same time there were instances where samples with higher solid phase concentrations were produced from noticeably lower aqueous concentrations. Examples of this occurred in the following examples: Red Oak and Leboskey had similar aqueous concentrations of Al yield vastly different solid concentrations (aqueous conc. 0.046 mg/L; solid conc. 88.3 mg/kg) compared to (aqueous conc. 0.048 mg/L; solid conc. 4,160 mg/kg), respectively. As previously mentioned the elevated concentration of Al in the solid phase Leboskey sample could be caused by clay contamination of the iron oxide sample, likely explaining this anomaly. Hartshorne (aqueous conc. 542 mg/L; solid conc. 572,070 mg/kg) and Red Oak (aqueous conc. 120 mg/L; solid conc. 592,150 mg/kg) had different concentrations of aqueous Fe lead to nearly similar solid phase concentrations. Hartshorne and Red Oak also displayed similar solid phase concentrations of Pb with a difference of an order of magnitude present in their aqueous concentrations (aqueous conc. 0.224 mg/L; solid phase conc. 206 mg/kg) compared to (aqueous conc. 0.039 mg/L; solid conc. 216 mg/kg), respectively. Interestingly, it should be noted that higher concentrations of Pb were

typically observed in iron oxides originating from coal mine discharges as compared to the iron oxides collected from the Mayer Ranch lead-zinc mine water discharge. Kairies et al. (2005) reports seeing large discrepancies (10 to 15 fold differences) between the aqueous concentration of Mn and the solid phase concentration. Large variations in solid phase Mn concentrations were also observed in this study with Leboskey being 22 times higher than Mayer Ranch, while each exhibited aqueous Mn concentrations slightly under 2.0 mg/L. Another interesting result resides in the fact that aqueous Cr concentrations at the Leboskey passive treatment system were found to be below detection limits (0.001 mg/L), yet in the precipitates collected from this system 6.35 mg/kg of Cr were present.

In addition to this, the Zn concentrations in the solid phase Mayer Ranch samples were an order of magnitude larger than the next highest sample. This elevated level of Zn was also seen in the aqueous Zn concentrations from these hard-rock mine water discharges. The Zn concentration of the mine water at Mayer Ranch is around 10 mg/L, while the next highest location is the Gowen Battles Seep with a concentration near 1 mg/L. This large difference in aqueous Zn concentrations lies in the fact that the Mayer Ranch site is located in an area that was mined for Pb and Zn, while the rest of the mine water discharges were of coal mining origin.

Conclusions

Mine drainage derived iron oxides are principally composed of a poorly ordered goethite due to the long aging time that is experienced after the mine water comes in contact with the atmosphere. It is evident from XRD and SEM analysis that over time, meta-stable forms of iron oxide such as ferrihydrite, lepidocrocite, and schwertmannite preferentially transform into more stable crystalline forms of iron oxide such as goethite. Additionally, iron content for mine drainage derived iron oxides was found to average over 72% as goethite, reaching a maximum of 94% as goethite. Site-specific water quality parameters such as mine water discharge pH, oxidative conditions, temperature, alkalinity, as well as sulfate and aqueous metals concentrations are influential in determining the physical properties of iron oxides that will be present in a given discharge. pH appears to be a controlling factor with respect to the extent that physical parameters of particle density and crystallinity are observed. Mine water discharges with lower pH's were generally seen to have both higher crystallinity and higher particle densities than those discharges with higher pH levels.

This study also supported the previous observations of Kairies et al. (2005) in which it was found that even though a particular metal is present in solution, it is not always a good indication of the concentration existing in the recovered iron oxide precipitates. It has been observed in this study that similar aqueous concentrations can yield vastly different solid phase concentrations (Al and Mn), while in other situations non-detectable aqueous concentrations of a dissolved metal such as Cr can hyper-accumulate in iron oxide precipitates. This level of unpredictability is most likely associated with the sorptive properties of mine drainage derived iron oxides and the relationship to their specific point of zero charge (pzc). The extent various ions are sorbed to iron oxides is heavily dependent on the surface area (as well as number of available binding sites) and the inherent pzc that each iron oxide possesses. The pzc is largely controlled by impurities incorporated into each iron oxides' structure, with pure samples of synthetic goethite having a pzc between 7.5 and 9 (Yates and Healy, 1975).

Future Research

Ongoing research in the form of laboratory scale sorption batch experiments using the iron oxide samples from this study, are being performed to evaluate the potential reuse of these iron oxides as a sorptive filtration media or coatings. Particular emphasis will be given to the monitoring of potential desorption of contaminants already associated with the iron oxides. These batch experiments are designed to evaluate the efficiency with which the chosen iron oxides remove phosphorus, arsenic, and zinc from polluted waters; thus assessing the feasibility of sustainably reusing of mine drainage derived iron oxides for water treatment purposes.

Acknowledgments

Special thanks go to the OU Center for the Restoration of Ecosystems and Watersheds, Dr. Madden and OU Physical and Environmental Geochemistry Laboratory, as well as Dr. Larson and OU Samuel Roberts Noble Electron Microscopy Laboratory for their willingness to participate in sample analyses and for the availability of their laboratory equipment. This work was partially supported by U.S. Environmental Protection Agency Agreements FY04 104(b)(3) X7-97682001-0, U.S. Geological Survey Agreement 04HQAG0131, and the University of Oklahoma Office of the Vice-President for Research, Institute for Oklahoma Technology Applications and Center for Restoration of Ecosystems and Watersheds.

Literature Cited

- American Public Health Association (APHA). 2005. Standard Methods for the Examination of Water and Wastewater. 21st Edition. American Public Health Association.
- Avotins, P.V.. 1975. Adsorption and Coprecipitation Studies of Mercury on Hydrous Iron Oxide. Ph. D. thesis, Stanford University, Stanford California.
- Ben-Dor, E., and A. Banin. 1989. Determination of organic matter in arid-zone soils using a simple "loss-on-ignition" method. *Commun. Soil Sci. Plant Anal.* 20:1675-1695. <http://dx.doi.org/10.1080/00103628909368175>.
- Bigham, J.M., Schwertmann, U. and Carlson, L., 1992. Mineralogy of precipitates formed by the biogeochemical oxidation of Fe(II) in mine drainage. *Catena Suppl.* 21, 219-232.
- Boujelben, N., Bouzid, J., et al. 2008. Phosphorus removal from aqueous solution using iron coated natural and engineered sorbents. *Journal of Hazardous Materials.* 151: 103-110. <http://dx.doi.org/10.1016/j.jhazmat.2007.05.057>.
- Brunauer, S., Emmett, P.H., and Teller, E. (1938) *J. Amer. Chem. Soc.* 60, 309. <http://dx.doi.org/10.1021/ja01269a023>.
- Cornell, R. M., and U. Schwertmann. 2003. *The Iron Oxides – Structure, Properties, Reactions, Occurrences, and Uses.* 2nd edition. Wiley-VCH Verlag GmbH and Co. KGaA, Weinheim.
- Crosby, S. A. et al.. 1983. Surface Areas and Porosities of Fe(III)- and Fe(II)- Derived Oxyhydroxides. *Environmental Science and Technology.* 17:709-713. <http://dx.doi.org/10.1021/es00118a004>.
- Domingo, C., Rodri'guez-Clemente, R., Blesa, M., 1994. Morphological properties of α -FeOOH, γ -FeOOH and Fe₃O₄ obtained by oxidation of aqueous Fe(II) solutions. *Journal of Colloid and Interface Science.* 165, 244–252. <http://dx.doi.org/10.1006/jcis.1994.1225>.
- Dzombak, David A., and Francois M. M. Morel. 1990. *Surface Complexation Modeling Hydrous Ferric Oxide.* John Wiley & Sons Inc. New York.
- Fenton, O., Healy, M. G., Rodgers, M., and D. O Huallacha`in. 2009. Site-specific P absorbency of ochre from acid mine-drainage near an abandoned Cu-S mine in the Avoca_Avonmore catchment, Ireland. *Clay Minerals.* Vol. 44. pp 113–123. <http://dx.doi.org/10.1180/claymin.2009.044.1.113>.

- Heal K. V., K. E. Dobbie, E. Bozika, H. McHaffie, A. E. Simpson, and K. A. Smith. 2005. Enhancing Phosphorus Removal in Constructed Wetlands with Ochre from Mine Drainage Treatment. *Water Science & Technology*. IWA Publishing. 51.9: 275-282.
- Hedin, R.S., 1996. Recovery of iron oxides from polluted coal mine drainage. Technical proposal for a patent application filed with the U.S. Patent and Trademark Office, pp. 1-32.
- Hedin, Robert. S.. 2002. Recovery of Marketable Iron Oxide from Mine Drainage. American Society of Mining and Reclamation.
<https://doi.org/10.21000/JASMR02010517>
- Hedin, Robert. S.. 1999. Recovery of Iron Oxides from Polluted Coalmine Drainage. Patent No. 5,954,969. U.S. Patent and Trademark Office, Washington D.C..
- Kairies, C. L., Capo, R. C., and G. R. Watzlaf. 2005. Chemical and physical properties of iron hydroxide precipitates associated with passively treated coal mine drainage in the Bituminous Region of Pennsylvania and Maryland. *Applied Geochemistry*. 20, 1445–1460.
<http://dx.doi.org/10.1016/j.apgeochem.2005.04.009>.
- Kang, Suck-Ki, Kwang-Ho Choo, and Kwang-Hee Lim. 2003. Use of Iron Oxide Particles as Adsorbents to Enhance Phosphorus Removal from Secondary Wastewater Effluent. *Separation Science and Technology*. 38:15. pp 3853 - 3874.
- Klute, A. 1986. *Methods of Soil Analysis, Part 1- Physical and Mineralogical Methods*. Second Edition. SSSA Book Series No. 5. American Society of Agronomy Inc. and Soil Science Society of America Inc. Madison, WI.
- Miot, J., K. Benzerara, G. Morin, A. Kappler, S. Bernard, M. Obst, C. Ferard, F. Skouri-Panet, J. M. Guigner, N. Posth, M. Galvez, G. E. Brown Jr., F. Guyot. 2009. Iron biomineralization by anaerobic neutrophilic iron-oxidizing bacteria. *Geochimica et Cosmochimica. Acta* 73. pp 696-711. <http://dx.doi.org/10.1016/j.gca.2008.10.033>.
- Munsell Color. 2000. *Munsell Soil Color Charts. Year 2000 Revised Washable Edition*. GretagMacbeth, Inc. New Windsor, NY.
- Nairn, R.W., T. Beisel, R.C. Thomas, J. Labar, K. Strevett, D. Fuller, W.H. Strosnider, W.J. Andrews, J. Bays, R.C. Knox. 2009. Challenges in Design and Construction of a Large Multi-Cell Passive Treatment System for Ferruginous Lead-Zinc Mine Waters. *Proceedings America Society of Mining and Reclamation*, 2009 pp 871-892.
<http://dx.doi.org/10.21000/JASMR09010871>.

- Penn, C.J., R.B. Bryant, and P.A. Kleinman. 2007. Sequestering dissolved phosphorus from ditch drainage water. *Journal of Soil Water Conservation*. 62:269-272.
- Schwertmann, U., and R. M. Cornell. 1991. *Iron Oxides in the Laboratory: Preparation and Characterization*. VCH Publishers Inc. New York.
- Sibrell, Philip L., Montgomery, Gary A., Ritenour, Kelsey L., and Travis W. Tucker. 2009. Removal of phosphorus from agricultural wastewaters using adsorption media prepared from acid mine drainage sludge. *Water Research*. Vol. 43. pp. 2240-2250. <http://dx.doi.org/10.1016/j.watres.2009.02.010>.
- U. S. Environmental Protection Agency (EPA). 2009. Test Methods for Evaluating Solid Waste, Physical/Chemical Methods. SW-846 (on-line). 3rd Edition. Office of Solid Waste, Washington D.C.. http://www.epa.gov/epawaste/hazard/testmethods/sw846/online/3_series.htm.
- Watzlaf, G.R., K.T Schroeder, R.L.P. Kleinmann, C.L. Kairies and R.W. Nairn. 2004. *The Passive Treatment of Coal Mine Drainage*. DOE/NETL-2004/1202. National Technical Information Service, Springfield, VA, pp 72.
- Wei, Xinchao, Viadero Roger C. Jr., and Shilpa Bhojappa. 2008. Phosphorus removal by acid mine drainage sludge from secondary effluents of municipal wastewater treatment plants. *Water Research*. Vol. 42. pp 3275-3284. <http://dx.doi.org/10.1016/j.watres.2008.04.005>.
- Wildeman, T. R., Spotts, E., Schafer, W. and J. Gusek. 1994. *Characterization, Management and Treatment of Water for Metal-Mining Operations*. Short Course at the 1994 Meeting of the American Society for Surface Mining and Reclamation. Pittsburgh, PA.
- Wiseman, I. M., and P. J. Edwards. 2004. *Constructed Wetland for Mine Water Treatment: Performance and Sustainability*. *The Journal*. Vol. 18, No. 3. pp 127-132.
- Yates, D.E., Healy, T.W., 1975. Mechanism of anion sorption at the ferric and chromic oxide/water interfaces. *Journal of Colloid and Interface Science*. 52, 222–228. [http://dx.doi.org/10.1016/0021-9797\(75\)90192-7](http://dx.doi.org/10.1016/0021-9797(75)90192-7).
- Yu, Ming-Ho. 2005. *Environmental Toxicology Biological and Health Effects of Pollutants*. CRC Press, Second Edition.